OCTOBER 1981

PPPL-1844
UC-20F

ION TEMPERATURE VIA LASER SCATTERING ON ION BERNSTEIN WAVES

BY

G.A. WURDEN, M. ONO, K.L. WONG

PLASMA PHYSICS LABORATORY

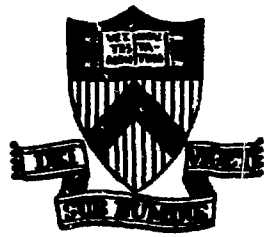

PRINCETON UNIVERSITY
PRINCETON, NEW JERSEY

This work was supported by the U.S. Department of Energy Contract No. DE-AC02-76-CHO 3073. Reproduction, translation, publication, use and disposal, in whole or in part, by or for the United States government is permitted.

Submitted to R&P
September 24, 1981

Ion Temperature Via Laser Scattering on Ion Bernstein Waves*

C. A. Wurden, M. Ono, K. L. Wong

Plasma Physics Laboratory, Princeton University
Princeton, New Jersey 08544

ABSTRACT

Hydrogen ion temperature has been measured in a warm toroidal plasma with externally launched ion Bernstein wave detected by heterodyne CO_2 laser scattering. Radial scanning of the laser beam allows precise determination of $k_\perp$ for the finite ion Larmor radius wave ($k_\perp \rho_i \sim 2$). Knowledge of the magnetic field strength and ion concentration then give a radially resolved ion temperature from the dispersion relation. Probe measurements and Doppler broadening of ArII 4806Å give excellent agreement.

Coherent light scattering from plasmas has been shown to be a powerful diagnostic tool, having previously been employed to observe driven electron Bernstein waves,[1] driven ion acoustic waves,[2-4] driven lower hybrid waves,[5] and, with a considerable degree of difficulty, the spectrum of thermal fluctuations to measure T_e/T_i.[6] This last measurement is generally recognized to require a pulsed, high power (Megawatt) laser of good spectral mode purity and a very sensitive broadband (~1 GHz) heterodyne detector for hydrogen ion temperature (T_i) measurement in a medium density (10^{13} - 10^{14} cm^{-3}) hot transient plasma.[7] The present paper demonstrates the first use of low power CW CO_2 laser scattering to detect externally launched ion Bernstein (IBW) test waves giving a nonperturbing measurement of the ion temperature in a warm, low density (T_i ~ 1.5 eV, T_e ~ 2 eV, n_e ~ 3×10^{10} cm^{-3}) hydrogen plasma.

The appropriate electrostatic dispersion relation for $\omega = \mathcal{O}(\Omega_i)$ is[8]

$$k_\perp^2 K_{xx} + k_\parallel^2 K_{zz} = 0 \ , \qquad (1)$$

where

$$K_{xx} = 1 + \sum_\sigma \omega_{p\sigma}^2 \exp(-b_\sigma) b_\sigma^{-1} \sum_{n=1}^{\infty} I_n(b_\sigma) \frac{2n^2}{(n^2\Omega_\sigma^2 - \omega^2)} \ ,$$

$$K_{zz} = 1 + 2(\omega_{pe}^2/\omega^2) y^2 [1 + y Z(y)] \simeq - \omega_{pe}^2/\omega^2 \ ,$$

and $b_\sigma \equiv k_\perp^2 T_\sigma / m_\sigma \Omega_\sigma^2$, σ denotes species, I_n is the modified Bessel function, $y \equiv (\omega/k_\parallel)(m_e/2T_e)^{1/2}$, and Z is the plasma dispersion function. Under the assumptions that $\omega^2 \ll \omega_{pi}^2$, $y \gg 1$ to avoid electron Landau damping and $k_\perp/k_\parallel \gg (m_i/m_e)^{1/2}$ so that the second term in Eq. (1) is negligible, the perpendicular wave phase velocity is in general proportional to the ion thermal velocity. In particular, for a single ion species plasma, and $\omega \lesssim 2\Omega_i$ we have

$$\lambda_\perp \simeq V_{Ti} \; f^{-1} \; (3/[4(\omega_i^2/\omega^2)-1])^{1/2} , \qquad (2)$$

where f is the wave frequency, $V_{Ti} = (T_i/m_i)^{1/2}$, having used a small argument expansion for $I_2(b_i)$. Eq. (2) clearly shows the dependence of IBW perpendicular wavelength $\lambda_\perp$ on the local ion temperature and magnetic field. Since the IBW is associated with ion motion in the bulk of the ion distribution function, the temperature obtained from the real part of the dispersion relation [Eq. (1)] is only weakly affected by possible fast tail components.

The experiment was performed in the steady-state ACT-1 (Advanced Concepts Torus) filament produced hydrogen plasma, of major radius R_o = 59 cm and minor radius r_o = 9 cm, but limited by adjustable vertical copper limiters. A schematic of the machine geometry is shown in Fig. 1(a). The pure toroidal magnetic field (B_o = 4.62 kilogauss on axis) was measured as a function of minor radius to $\pm$ 1/4% accuracy with a Bell Model

615 Hall effect gaussmeter. H_2 neutral fill pressure can be lowered to an absolute 2×10^{-5} torr, with a base pressure $\sim 5 \times 10^{-7}$ torr, resulting in a $T_e \approx T_i \leq 2$ eV hydrogen plasma. The wave is excited by two external (R = 65.5 cm) 12 cm high $\times$ 5 cm wide vertical flat plate IBW antennas, spaced 17 cm apart and driven 180° out of phase to define $\lambda_{\parallel} \sim 34$ cm.[9]

The laser system [see Fig. 1(b)] consists of a single mode 50 watt continuous wave (CW) CO_2 laser at $\lambda_o = 10.6$ μm, used in conjunction with a liquid helium cooled copper-doped germanium .5 mm $\times$ .5 mm photoconductor, configured in a small angle (3-26 milliradian) forward scattering geometry. Both the .1 watt local oscillator and high power (~20-30 watts typical) laser beam are focussed and crossed in the plasma for ease of alignment.[10] Their intersection, along approximately vertical chords, defines the Bragg scattering angle $\theta_B = 2 \arcsin (\lambda_o / 2\lambda_B)$, which can be scanned by translating mirror M5. Their matched Gaussian beam waists (radius at $1/e^2$ power point) a_o 3.3 mm in the plasma give an angle defined k-resolution $\Delta k_\perp = 2/a_o \sim 6$ cm^{-1}. Isolation of the detector electronics (~70 db gain) is a major concern and is achieved through careful RF shielding, battery supplies, and a wideband (140 MHz) analog fiber optic link to the outside world. The resulting system noise equivalent power in the frequency band of interest (9-13 MHz) at the fiber optic receiver is NEP $\sim 2 \times 10^{-18}$ W/Hz, as determined by black body and gain-recombination noise measurements.[11] Density fluctuation levels $\tilde{n}$, given uniform wave

phase fronts along the scattering volume, can be estimated according to[12]

$$\frac{P_s}{P_i} = \frac{1}{4} r_o^2 \lambda_o^2 (\tilde{n}L)^2,$$

where P_s is the scattered laser power, P_i the incident laser power, r_o is the classical electron radius, and L the effective length of the scattering volume along the beam. Observed fluctuation levels at the pump frequency range from $\tilde{n} \sim 5 \times 10^5$ cm^{-3} to 1×10^8 cm^{-3} with RF powers of .005 - 2 watts, and lock-in times of0.3-1.2 seconds, under varying plasma and antenna conditions. It should be noted that the largest signals can be seen directly on a spectrum analyzer without using a lock-in.

An interesting feature of this scattering system is that it can be continuously driven during a measurement across the outer minor radius of the plasma at constant scattering angle. A Princeton Applied Research 5202 50 MHz bandwidth lock-in allows direct interferometry (in the RF sense) of the IBW signal. Phase information is contained in the oscillating heterodyne photocurrent $I_{\ell s}$[10]

$$I_{\ell s} \propto \tilde{n} \exp[-(k_\perp - k_B)^2 a_o^2/8] \cos(k_\perp x_o),$$

for $k_\perp \approx k_B$, where $k_B = 2\pi/\lambda_B$, x_o is in the direction of the major radius, and $\tilde{n}$ is the amplitude of the fluctuating component of the electron density at the pump frequency with perpendicular wavenumber $k_\perp$. By scanning x_o a very accurate measurement of

$k_\perp$ similar to probe interferometry in the case of a long wavetrain, as in Fig. 2(a), can be obtained. In Fig. 2(b) we show a comparison of a twin tip microcoaxial floating probe signal (tips ||B) with the laser heterodyne photocurrent at a 12.3 MHz IBW frequency. Notice the better sensitivity of the laser at short wavelengths relative to the probe. As we show later, good agreement is obtained between the dispersion relation measured by the probe and laser.

Radial ion temperature profiles can be readily obtained through measurement of the local IBW perpendicular wavelength. In Fig. 3(a) we show calculated curves of $\lambda_\perp$ vs. radius r at different ion temperatures (using an independently measured abundance of H_1^+ ~ 50% ± 5%,[9] remainder being H_2^+, H_3^+ at this fill pressure) and data points from a single laser waveform at f = 12.4 MHz (3.5 watt RF power). Then in Fig. 3(b) we plot T_i vs r at two hydrogen neutral fill pressures, as seen by laser and probe. Central ion temperature is observed to scale approximately inversely with neutral fill pressure.

We have run an independent Fabry-Perot ion temperature measurement with a mixed Argon-Hydrogen plasma. At a measured 20% H^+ concentration, a simultaneous comparison between the argon bulk ion energy, as inferred from the full width half max Doppler line width of the π component of singlet ArII 4806Å averaged along a central vertical chord, and the IBW derived hydrogen ion temperature, showed agreement to within 10%. This measurement used a pressure-scanned Fabry-Perot in conjunction with a grating prefilter.[13]

Higher harmonic IBW in pure hydrogen can also be observed, both of the major ion species H_1^+, and of H_2^+, H_3^+. These three species effectively model H^+, D^+, T^+ with regard to resonances in the IBW dispersion relation. In Fig. 4 we see a more complete portion of the IBW dispersion relation, showing up to the 4th harmonic of H_1^+ [Fig. 4(a)], and clear indications of the 8th harmonic of H_3^+ [Fig. 4(b)]. The effects of a multispecies plasma are evident in Fig. 4(c). Here the theoretical curves give a best fit H_1^+: H_2^+: H_3^+ in ratio $50 \pm 3 : 28 \pm 2 : 22 \pm 2$, in agreement with independent N_i measurements, yielding one ion temperature $T_i = 1.35 \pm .2$ eV for all three species, as expected from estimated ion equilibration times <50 μsec. The second harmonic IBW of H_1^+ and lower frequency branches are particularly insensitive to n_e and $k_\parallel$ and allow a good determination of T_i and relative concentrations.

In summary, we have successfully measured radial hydrogen ion temperature profiles using laser scattering to determine the perpendicular wavelength of an externally launched ion Bernstein test wave. A variant of this ion temperature diagnostic technique (using far infrared laser or microwave scattering) could complement existing ones on tokamaks, since it does not rely on the presence of impurities, neutrals, or hot ion tails, (and may even yield ion concentration information deep inside the plasma core).[14]

The authors would like to thank C. M. Surko and R. E. Slusher for valuable advice early on in the scattering setup, E. Tolnas for help with the Fabry-Perot, and J. Taylor and W. Kineyko for their invaluable technical support.

This work supported by the U.S. Department of Energy Contract No. DE-AC02-76-CHO3073.

REFERENCES

[1]C. M. Surko, P. E. Slusher, D. P. Moler, M. Porkolab, Phys. Rev. Lett. 29, 81 (1972).

[2]D. R. Baker, N. R. Beckenberg, J. Meyer, Phys. Lett. 51 A, 185 (1975).

[3]A. L. Peratt, R. L. Watterson, H. Oerfler, Phys. Fluids 20, 1900 (1977).

[4]H. Park, W. A. Peebles, A. Mase, N. C. Luhmann Jr. A. Semet, Appl. Phys. Lett. 37, 279 (1980).

[5]C. M. Surko, R. E. Slusher, J. J. Schuss, et al., Phys. Rev. Lett. 43, 1016 (1979).

[6]E. Holzhauer, Phys. Lett. 62 A, 495 (1977).

[7]A. Gondhalekar, P. Keilmann, Opt. Commun. 14, 263 (1975).

[8]M. Ono, K. L. Wong, Phys. Rev. Lett. 45, 1105 (1980).

[9]M. Ono, K. L. Wong, G. A. Wurden, Princeton Plasma Physics Laboratory Report No. 1819 (July 1981).

[10]R. E. Slusher, C. M. Surko, Phys. Fluids 23, 3 (1980).

[11]F. R. Arams, E. W. Sard, J. B. Peyton, F. P. Pace, IEEE J. Quan. Elec. QE-3, 484 (1967).

[12]L. D. Landau, E. M. Lifshitz, Electrodynamics of Continuous Media, 399 (Pergamon, New York, 1960).

[13]J. G. Hirschberg, E. L. Wilson, Princeton Plasma Physics Laboratory Report MATT-562 (Nov. 1968).

[14]G. A. Wurden, M. Ono, K. L. Wong, A. Semet, Bull. Am. Phys. Soc. 25, 938 (1980).

FIGURE CAPTIONS

Fig. 1. (a) Schematic of the experimental apparatus. (b) Diagram of the laser scattering geometry. Mirrors M6 and M7 move with the optics table.

Fig. 2. (a) Schematic of IBW propagation, launched from external electrostatic plate antennas. (b) Comparison of detected IBW perpendicular waveforms at f = 12.3 MHz, 1.8 watts RF, neutral fill pressure P = 4×10^{-5} torr. The antennas are at r = 6.5 cm.

Fig. 3. Radial hydrogen ion temperature determination. (a) Computer generated constant T_i curves, and measured laser points at f = 12.4 MHz, $N_{H_1^+}$ = 50%, P = 2.5×10^{-5} torr, $\lambda_\perp$ = 34 cm, T_e = 2 eV, $n_{eo} = 3.5 \times 10^{10}$ cm^{-3}. (b) Comparison of radial temperature profiles obtained by laser (circles) and probe (triangles) from single frequency waveforms, at two neutral fill pressures.

Fig. 4. Ion Bernstein wave dispersion relation, hydrogen plasma. Laser points (O), probe points (▲), using internal grid excitation. Data taken at r = 1.5 cm, $n_e = 2.4 \times 10^{10}$ cm^{-3}, P = 2.5×10^{-5} Torr, $\Omega_{H_1^+}/2\pi$ = 6.83 MHz, T_e = 2 eV, $\lambda_\perp \sim 130$ cm. Theoretical curves at two T_i values bracket data points. (a) 4th harmonic IBW branch of H_1^+. (b) 3rd harmonic of H_1^+, and evidence of 8th of H_3^+. (c) Second harmonic IBW branch used for T_i, and lower frequency branches for H_2^+, H_3^+ concentrations.

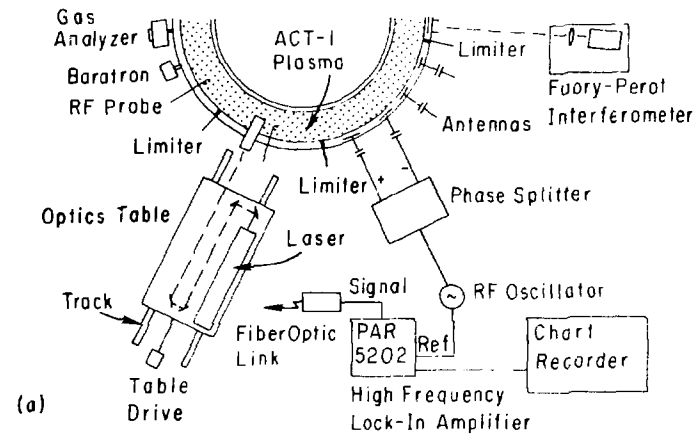
Gas Analyzer
Baratron
RF Probe
Limiter
ACT-I Plasma
Limiter
Limiter
Antennas
Fabry-Perot Interferometer
Optics Table
Laser
Track
Table Drive
Signal
FiberOptic Link
PAR 5202
Ref
RF Oscillator
Phase Splitter
Chart Recorder
High Frequency Lock-In Amplifier
(a)

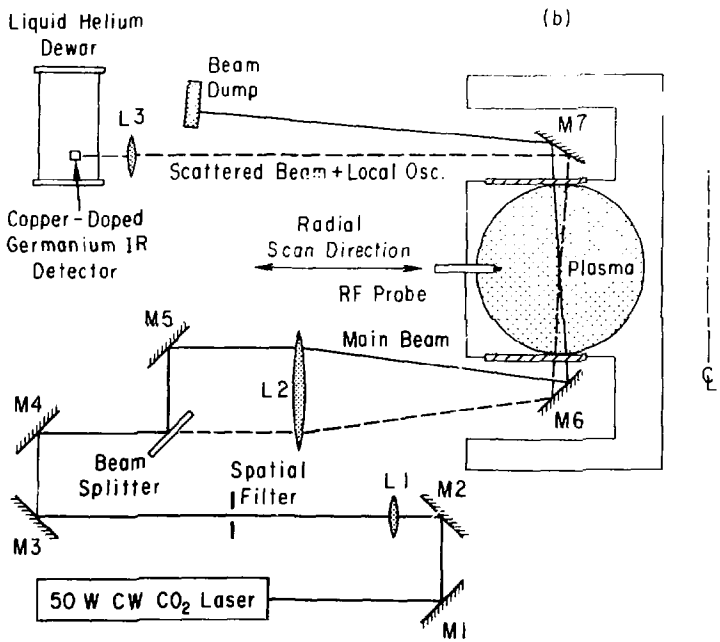
(b)
Liquid Helium Dewar
Beam Dump
L3
Scattered Beam + Local Osc.
Copper-Doped Germanium IR Detector
Radial Scan Direction
RF Probe
M7
Plasma
M5
Main Beam
L2
M4
M6
Beam Splitter
Spatial Filter
L1
M2
M3
50 W CW CO_2 Laser
M1

FIGURE 1

81X1104

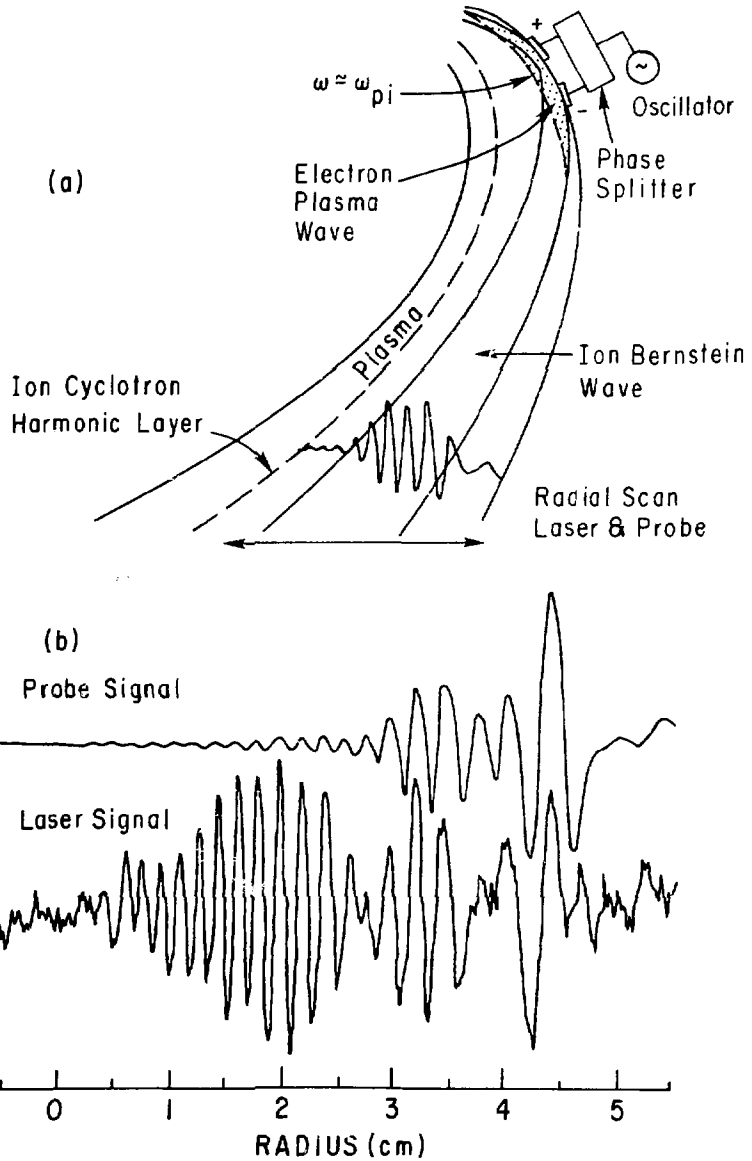

FIGURE 2

81X1101

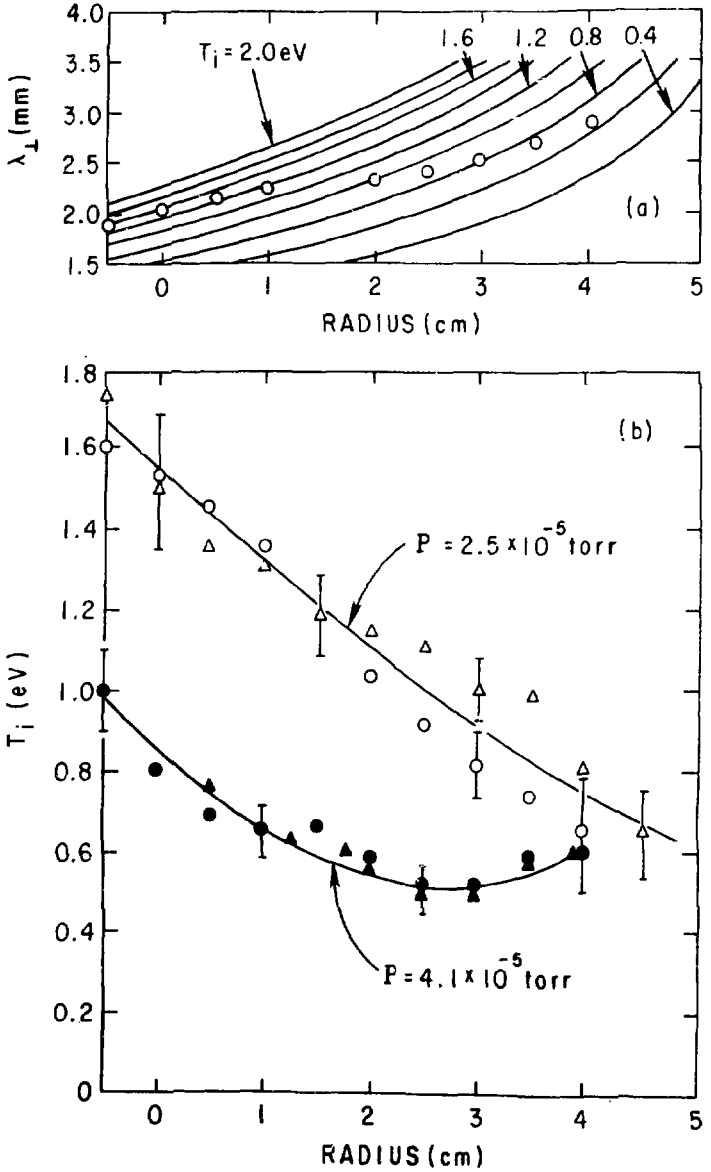

FIGURE 3

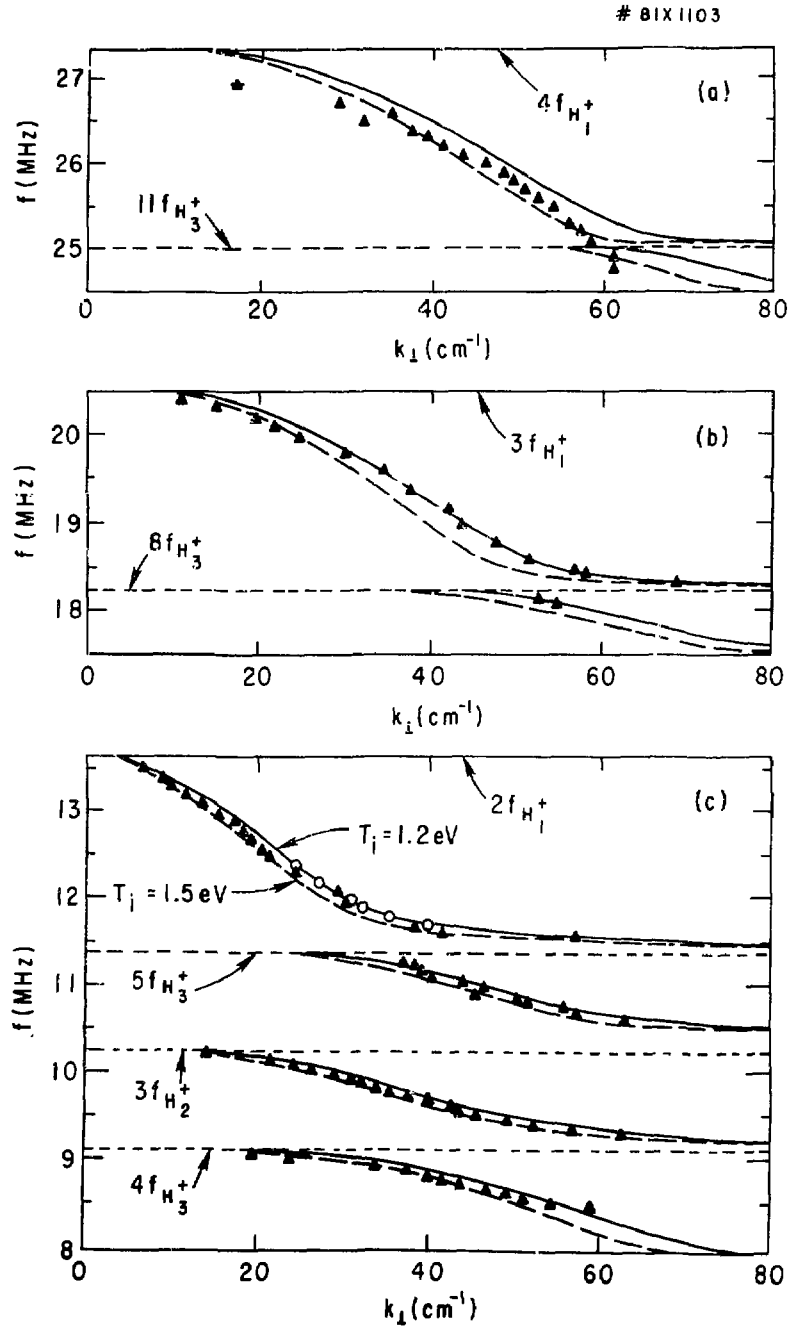
81X1103
(a)
$4f_{H_1^+}$
$11f_{H_3^+}$
f (MHz)
27
26
25
0
20
40
60
80
$k_\perp (cm^{-1})$
(b)
$3f_{H_1^+}$
$8f_{H_3^+}$
f (MHz)
20
19
18
0
20
40
60
80
$k_\perp (cm^{-1})$
(c)
$2f_{H_1^+}$
$T_i = 1.2 eV$
$T_i = 1.5 eV$
$5f_{H_3^+}$
$3f_{H_2^+}$
$4f_{H_3^+}$
f (MHz)
13
12
11
10
9
8
0
20
40
60
80
$k_\perp (cm^{-1})$

FIGURE 4